



Weld Shape Variation and Electrode Oxidation Behavior under Ar-(Ar-CO₂) Double Shielded GTA Welding

Shanping Lu^{1)†}, Hidetoshi Fujii²⁾ and Kiyoshi Nogi²⁾

1) Shenyang National Laboratory for Materials Science, Institute of Metal Research, Chinese Academy of Science, Shenyang 110016, China

2) Joining and welding Research Institute, Osaka University, Osaka 567-0047, Japan

[Manuscript received September 22, 2008, in revised form February 20, 2009]

Double shielded gas tungsten arc welding (GTAW, also known as tungsten inert gas (TIG) welding) of an SUS304 stainless steel with pure inert argon as the inner layer shielding and the Ar-CO₂ or CO₂ active gas as the out layer shielding was proposed in this study to investigate its effect on the tungsten electrode protection and the weld shape variation. The experimental results showed that the inner inert argon gas can successfully prevent the outer layer active gas from contacting and oxidizing the tungsten electrode during the welding process. Active gas, carbon dioxide, in the outer layer shielding is decomposed in the arc and dissolves in the liquid pool, which effectively adjusts the active element, oxygen, content in the weld metal. When the weld metal oxygen content is over 70×10^{-6} , the surface-tension induced Marangoni convection changes from outward into inward, and the weld shape varies from a wide shallow one to a narrow deep one. The effect of the inner layer gas flow rate on the weld bead morphology and the weld shape was investigated systematically. The results show that when the flow rate of the inner argon shielding gas is too low, the weld bead is easily oxidized and the weld shape is wide and shallow. A heavy continuous oxide layer on the liquid pool is a barrier to the liquid pool movement.

KEY WORDS: Double shielding; Weld shape; Marangoni convection; Gas tungsten arc welding

1. Introduction

Gas tungsten arc welding (GTAW), also known as tungsten inert gas (TIG) welding has been widely used in industry for its high weld quality especially for stainless steel, titanium alloys and non-ferrous alloys. However, its shallow penetration makes the weld depth/width ratio only around 0.2 and causes lower weld production. How to increase the GTAW penetration has been concerned for a long time, and several technologies have been proposed including the adjustment to the minor elements in the raw material, such as S, O, Se and Bi in group VIB and F, Br and Cl in group VIIB^[1-8], smearing active fluxes on the plate surface (A-TIG or FB-TIG) before welding^[7,9-28], and

adding a small amount of active gas to the inert shielding gas^[29-35] to obtain a deep penetration. Even though some techniques have been partially applied in industry, there is still no common agreement on the mechanism of A-TIG welding. There have been four proposed mechanisms to explain the A-TIG phenomenon, including the TIG keyhole model^[36], arc contraction theory^[19-23,26,27,37,38], weld pool convection theory^[6,7,18,39-42] and flux insulation model^[43].

Since 2002, a series experimental research on high efficient GTA welding have been carried out by the present authors including smeared oxide fluxes on the plate before welding^[24,25], adding a small amount of the active gas, O₂ or CO₂, to the argon shielding gas^[32-34], and adding O₂ or CO₂ to the helium shielding gas^[44,45]. The results showed that the weld penetration can be significantly increased for SUS304 stainless steel by smearing an oxide flux or adding

† Corresponding author. Assoc. Prof. Ph.D.; Tel.: + 86 24 23971429; E-mail address: shplu@imr.ac.cn (S.P. Lu).

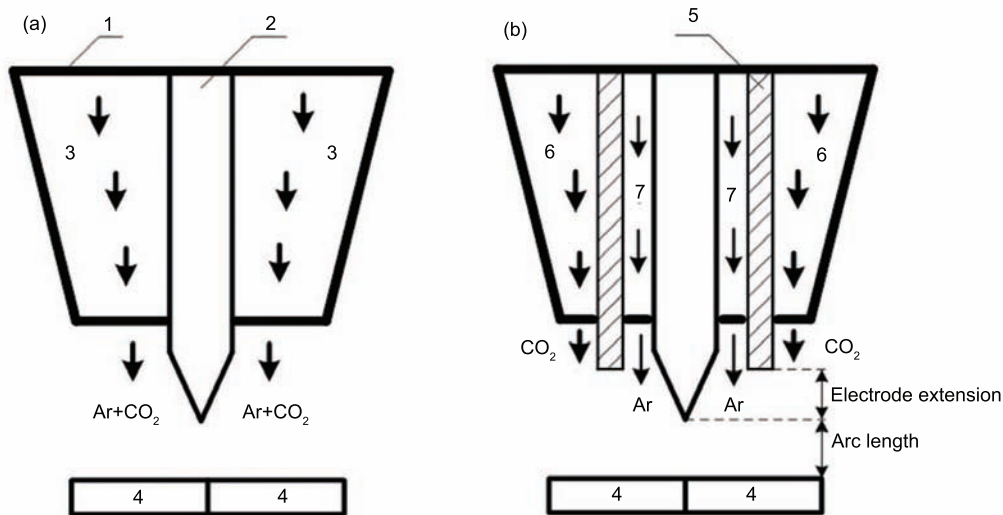


Fig. 1 Schematic diagram of TIG torch (a) and double shielding torch (b): 1—shield cap; 2—electrode; 3—mixed shielding gas; 4—substrate; 5—ceramic nozzle; 6—out layer shielding gas; 7—inner layer shielding gas

an active gas into inert shielding gas. The active element, oxygen, in the weld pool can be adjusted by smearing the oxide flux or adding a small amount of the active gas to the inner shielding. When the oxygen content is over a critical value, the reverse Marangoni convection is induced and a deep narrow weld shape is obtained. However, the weld shape is sensitive to the quantity of the smeared oxide flux before welding, and it is difficult for the operator to control the quantity of flux used. For the Ar (He)-O₂ (CO₂) mixed shielding, the addition of oxygen or carbon dioxide to the shielding oxidizes the tungsten electrode during long term application, which will shorten the electrode service life.

In order to protect the electrode from oxidation during the Ar (He)-O₂ (CO₂) mixed GTA welding, a new method, named as double shielded GTA welding, is proposed in this study to control the liquid pool movement and decrease the tungsten electrode oxidation rate as shown in Fig. 1(b). The pure argon was used as the inner layer shielding gas around the tungsten electrode to generate the arc and protect the electrode from oxidation. The outer layer gas, CO₂ or Ar-CO₂ mixture, was used around the inner shielding gas to adjust the active element content in the weld pool by the carbon dioxide decomposition and dissolution in the liquid pool during the welding process. The absorption rule of the active element from the outer layer shielding gas in the weld pool and its influence on the Marangoni convection, weld shape variation and electrode protection were described in this paper. The effect of the inner layer gas flow rate on the weld shape, bead morphology was also investigated systematically.

2. Experimental

SUS304 stainless steel with the dimension of

100 mm×50 mm×10 mm was used as the substrate with the average composition of 0.06%C, 0.44%Si, 0.96%Mn, 8.19%Ni, 18.22%Cr, 0.027%P, 0.0020%S and 0.0020%O and the rest of Fe. Prior to the welding, the surface of the plate was ground using an 80-grit flexible abrasive paper and then cleaned with acetone.

A water-cooled double shielded torch with a thoriated tungsten electrode (W-2%ThO₂, 2.4 mm in diameter) was used in the experiments by direct current, electrode negative (DCEN) polarity power source (YC-300BZ1) with a mechanized system, in which the test piece moves at a set speed. Figure 1 is the schematic diagram of TIG torch and the double shielding torch. For the common TIG torch (Fig. 1(a)), one mixed shielding gas (Ar-CO₂) was used. Figure 1(b) shows the double shielding torch used in this study with two layer shielding gases separated by a ceramic nozzle. The inner layer shielding gas is pure argon to generate arc and protect the electrode, and the outer layer shielding gas is CO₂ or Ar-CO₂ mixed shielding to adjust the oxygen content and Marangoni convection in the liquid pool during the welding process. The welding parameters are shown in Table 1. The out layer shielding gas flow

Table 1 Welding parameters

Parameters	Value
Electrode type	DCEN, W-2%ThO ₂
Diameter of electrode/mm	2.4
Vertex angle of electrode/deg.	30
Inner layer shielding gas	Ar
Inner layer gas flow rate/(L/min)	3–10
Out layer shielding gas	Ar-CO ₂ , CO ₂
Out layer gas flow rate/(L/min)	10
Electrode extension/mm	0–3
Arc length/mm	3
Welding current/A	160
Welding speed/(mm/s)	2

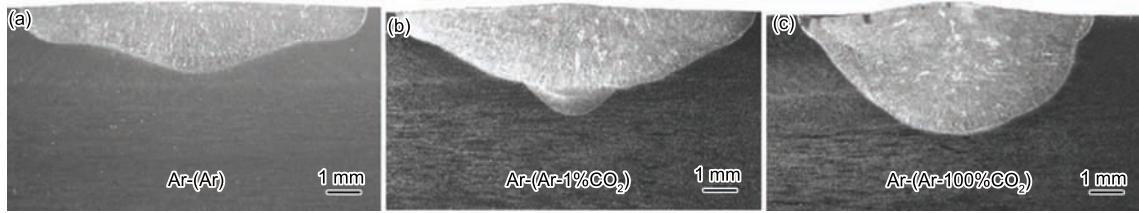


Fig. 2 Weld shapes with different out layer shielding gas

rate is 10 L/min. The effects of the inner layer shielding gas flow rate and electrode extension on the weld shape and bead morphology were also investigated under Ar-(CO₂) double shielding.

After welding, the weld bead and electrode morphologies were photographed. Then, all the weld beads were sectioned and the specimens for the weld shape observations were prepared by etching, a HCl (50 ml)+Cu₂SO₄ (25 ml) solution, to reveal the bead shape and dimensions. The cross-sections of the weld bead were photographed using an optical microscope. The oxygen content in the weld metal was analyzed using an oxygen/nitrogen analyzer (Horiba, EMGA-520). Samples for the oxygen measurements were cut directly from the weld metal.

3. Results and Discussion

3.1 Weld shape and electrode morphology

The effect of the outer layer gas composition on the weld bead shape and electrode morphology was studied with three different out layer shielding gas, pure Ar, Ar-1%CO₂ and pure CO₂, at 160 A welding current, 2 mm/s welding speed and 10 L/min flow rate for both the inner and outer layer shielding gases. Figure 2 shows the weld shapes with different out layer shielding gases. When using pure Ar or Ar-1%CO₂ as the out layer shielding gas, the weld shapes are wide and shallow as shown in Fig. 2(a) and (b). When the pure CO₂ is used as the outer layer shielding gas, the weld shape becomes relatively narrow and deep as shown in Fig. 2(c). The composition of the outer layer shielding gas can significantly affect the weld shape. Figure 3 compares the electrode morphologies under single layer Ar-CO₂ mixed shielding (Fig. 3(a) to (c)) with those under the double layer shielding (Fig. 3(d) to (f)). Under the single layer Ar-CO₂ mixed shielding with the common TIG torch (Fig. 1(a)), the electrode was oxidized seriously after welding, even though the carbon dioxide content in the shielding gas was below 3% as shown in Fig. 3(b) and (c). However, under double layer shielding with double shielded torch (Fig. 1(b)), the electrode was well protected as shown in Fig. 3(e) and (f) even though 100% carbon dioxide was used in the out layer shielding gas. In the double layer shielding, the inner layer

pure argon shielding gas well protected the electrode and successfully prevented the carbon dioxide in the out layer gas from contacting and oxidizing the tungsten electrode.

3.2 Oxygen absorption and Marangoni convection

Table 2 shows the effect of the out layer shielding gas composition on the weld depth/width (D/W) ratio and the weld metal oxygen content. When the pure argon or Ar-1%CO₂ are used as the out layer shielding, the weld metal oxygen contents are 27.2×10^{-6} and 43×10^{-6} , respectively, lower than 70×10^{-6} . When pure carbon dioxide is used as the out layer shielding, the weld metal oxygen content is over 70×10^{-6} . The weld D/W ratio increases from 0.19 and 0.28 to 0.41 when the weld metal oxygen content is over 70×10^{-6} . Carbon dioxide in the outer layer shielding gas will be decomposed in the high temperature arc and dissolve in the liquid pool during the welding process. Therefore, the weld metal oxygen content (active element) can be adjusted by the addition of the carbon dioxide in the outer layer shielding gas in the double shielded GTA welding.

Generally, the weld shape is controlled by heat transfer due to a combination of convection and conduction in the liquid pool. The relative importance between the heat convection and conduction, which can be determined by the Peclet number, varies for different materials and represents the ratio of heat transfer by convection and conduction. It is defined as follows: $Pe = L \cdot V_{\max} / 2\alpha_l$, where V_{\max} is the maximum surface velocity, α_l is the thermal diffusivity of liquid and L is the characteristic length of the weld pool, which can be taken as the weld pool surface radius for wide and shallow weld pool with or without a low active element content. In a deep and narrow weld pool containing certain active element, L can be taken as the depth of the weld pool^[33]. Here, two representative weld shapes, Fig. 2(a) and (c), are selected to calculate the Peclet number. The weld pool surface radius for Fig. 2(a) is 5.91 mm, and weld depth for Fig. 2(c) is 3.88 mm. The other thermal properties for SUS304 are from literature [33]. The calculated Peclet numbers are 90.9 and 59.7 for Fig. 2(a) and (c), respectively. Previous work by Limmaneevichitr and Kou^[46] showed that the heat transfer in the weld pool is dominated by conduction for $Pe \ll 1$, while

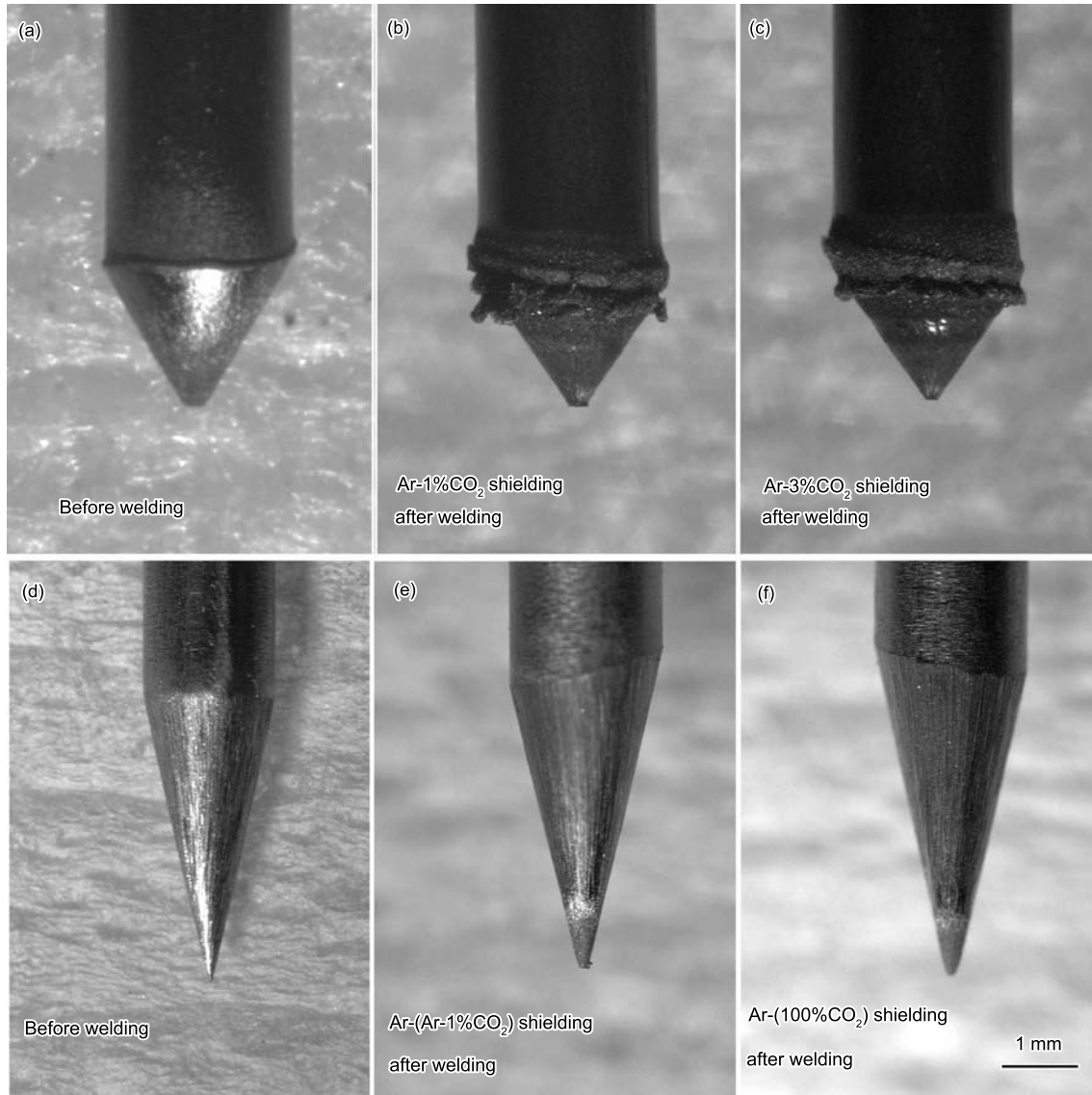


Fig. 3 Comparison of electrode oxidation under mixed shielding ((a)–(c)) and double shielding ((d)–(f))

Table 2 Weld depth/width (D/W) ratio and $[O]$ in weld metal under different out layer shielding gas

Inner layer gas	Out layer gas	Weld D/W ratio	$[O]$ in weld metal/ 10^{-6}
Pure Ar	Pure Ar	0.19	27.2
Pure Ar	Ar-1%CO ₂	0.28	43.0
Pure Ar	100%CO ₂	0.41	75.9

on the other hand, for $Pe \gg 1$, the heat transfer in the weld pool is dominated by convection. The high Peclet number signifies that the heat transfer in the liquid pool in this study is dominated by the convection mode. Therefore, the GTA weld shapes here depend to a large extent on the fluid flow mode in the welding pool, which was governed by the combined effect of the electromagnetic force, surface tension, buoyancy force and impinging force of the arc plasma.

Previous research works have shown that the Marangoni convection induced by the surface ten-

sion on the pool surface is the main convection that significantly influences the fluid flow in a liquid pool^[6,7,18,39–42,47,48]. Generally, the surface tension decreases with increasing temperature, that is $\partial\sigma/\partial T < 0$, for a pure metal and many alloys. Since there is a large temperature gradient on the welding pool surface, a large surface tension gradient arises along the surface. In the weld pool of such materials, the surface tension is higher at the cooler pool edges than that at the pool center. Hence, the Marangoni convection flows from the pool center to the edges. The heat flux from the arc is readily transferred from

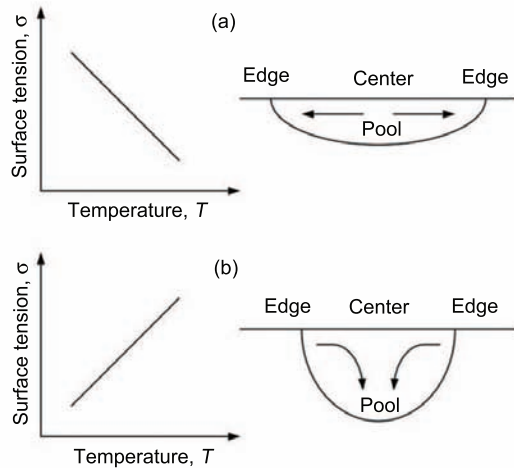


Fig. 4 Marangoni convection mode in the weld pool: (a) $\partial\sigma/\partial T < 0$, (b) $\partial\sigma/\partial T > 0$

the pool center to the edges and the weld shape becomes relatively wide and shallow as shown in Fig. 4(a).

Simulation research^[49] and experimental work^[50] on the temperature coefficient of the surface tension for the Fe-O binary metal showed that oxygen is a surface active element in the Fe-O system. The temperature coefficient of the surface tension ($d\sigma/dT$) is always negative for the Fe-O system with low oxygen content. On the other hand, it changes from negative to positive when the oxygen content is over a critical value. Heiple and Ropper^[6,7] and Lu *et al.*^[24,25,32–34] found that S and O are also active elements for stainless steel. When the active element content exceeds the critical value, the temperature coefficient of the surface tension ($d\sigma/dT$) changes from negative to positive, that is $d\sigma/dT > 0$, and the direction of the Marangoni convection on the weld pool changes in the manner as illustrated in Fig. 4(b). In this case, the heat flux transfers from the center to the bottom and a relatively deep and narrow weld shape forms. The previous experimental results^[24,25] showed that when the oxygen content in the weld pool ranges from 70×10^{-6} to 300×10^{-6} in SUS304 stainless steel, the temperature coefficient of the surface tension ($d\sigma/dT$) became positive.

The weld metal oxygen contents is over 70×10^{-6} when the pure carbon dioxide is used as the out layer shielding as shown in Table 2. In this case, the Marangoni convection direction changes from outward to inward. Therefore, the weld shape changes from a relatively wide and shallow type (Fig. 2(a) and (b)) to a narrow and deep one (Fig. 2(c)), and the weld depth/width ratio (D/W) suddenly increases from 0.28 to 0.41 when the pure carbon dioxide is used in the out layer shielding.

3.3 Effect of inner gas flow rate on the weld shape and bead morphology

The ratio between the inner layer gas flow rate

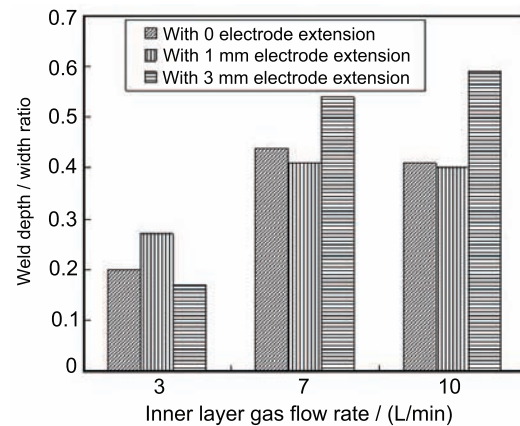


Fig. 5 Effect of inner layer gas flow rate on the weld depth/width ratio

(pure Ar) and the out layer shielding gas (pure CO_2) is one of the important parameters, which affects the active element, oxygen, dissolution in the weld pool, Marangoni convection, weld shape and the bead morphology. The outer layer shielding gas (CO_2) flow rate is set at 10 L/min here, and the inner layer shielding gas is varied from 3 to 10 L/min under different electrode extension from 0 to 3 mm. Figure 5 shows the effect of the inner layer gas flow rate on the weld depth/width ratio with different electrode extensions. The weld depth/width ratio is lower for the 3 L/min inner layer gas flow rate than those for the 7 and 10 L/min inner layer gas flow rates.

Figure 6(a) and (b) shows that the weld shape under the 3 L/min inner layer gas flow rate is wide and shallow and the weld bead is seriously oxidized. However, the weld shapes are narrow and deep with clean bead surfaces as shown in Fig. 6 (b) to (f) when the inner layer gas flow rates are 7 and 10 L/min. The weld metal oxygen analysis shows that the oxygen content in the weld metal for the 3 L/min flow rate is much higher (over 350×10^{-6}) than that (between 70×10^{-6} to 100×10^{-6}) for 7 and 10 L/min inner layer gas flow rates as shown in Fig. 7.

When the inner layer pure inert gas (argon) flow rate is too low, the percent of the out layer active gas (pure CO_2) is relatively high in the total shielding gas, which makes the weld bead oxidized easily during the welding process as shown in Fig. 6(d) and the weld metal oxygen content in the weld metal high (over 350×10^{-6}) as shown in Fig. 7. The heavy continuous oxide layer on the pool surface prevents the liquid pool from moving freely, and also changes the liquid pool/gas surface to the liquid pool/oxide layer interface. The surface tension induced inward Marangoni convection no longer exists at the interface and the weld shape becomes wide and shallow as shown in Fig. 6(a). For the 7 and 10 L/min inner pure inert gas shielding, the weld bead is clean and the weld metal oxygen is between 70×10^{-6} to 100×10^{-6} as shown in

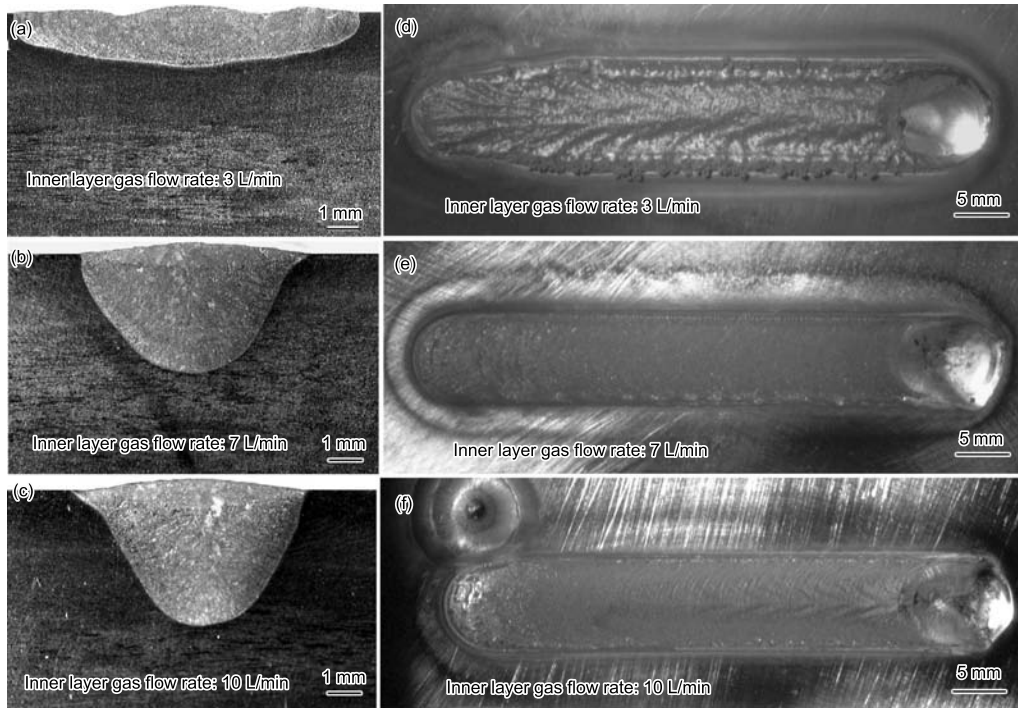


Fig. 6 Effect of inner layer gas flow rate on the weld shape and weld bead morphology

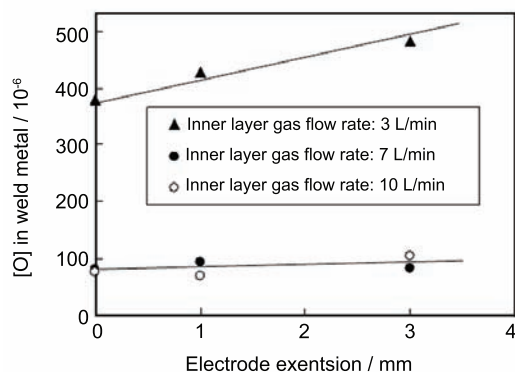


Fig. 7 Effect of the inner layer gas flow rate and electrode extension on the weld metal oxygen content

Fig. 7. In this case, an inward Marangoni convection exists, which makes the weld shapes narrow and deep as shown in Fig. 7(b) and (c).

4. Conclusions

(1) Double shielded GTA welding using the pure inert Ar gas as the inner layer shielding and the active CO₂ or Ar-CO₂ gas as the outer layer shielding can protect well the tungsten electrode from oxidation in the welding process. The inner layer Ar gas can effectively prevent the out layer active gas from contacting and oxidizing the tungsten electrode. The weld shape changes from a wide shallow one to a narrow deep one and the weld depth/width increases from 0.28 to 0.41 when the carbon dioxide is used as the out layer

shielding. Double shielded GTA welding is a method to improve the GTA welding production.

(2) The active gas, carbon dioxide, in the out layer shielding is decomposed and the active element, oxygen, dissolves in the liquid pool during the welding process, which successfully adjusts the active element content in the weld pool and controls the Marangoni convection mode on the pool surface. When the oxygen content in the liquid pool is over 70×10^{-6} , the outward Marangoni convection changes into an inward convection, and the weld shape varies from a wide shallow one to a narrow deep one.

(3) The flow rate ratio between the inner inert gas and the out active gas is an important welding parameter, which directly affect the weld shape and the weld bead morphology. When the inner layer gas flow rate is lower, the weld bead is seriously oxidized in the welding process and the weld shape is wide and shallow. A heavy continuous oxide layer on the liquid pool is a barrier to the liquid pool movement.

Acknowledgements

This work was supported by the National Science Foundation of China under Grant No. 50874101 and the Science Program of Shenyang City under Grand No. 1071275-0-02.

REFERENCES

- [1] H. Ludwig: *Weld. J.*, 1957, **36**, 335s.
- [2] W.F. Savage, E.F. Nippes and G.M. Goodwin: *Weld. J.*, 1977, **56**, 126s.

- [3] G.W. Oyler, R.A. Matuszesk and C.R. Carr: *Weld. J.*, 1967, **46**, 1006.
- [4] W.S. Bennett and G.S. Mills: *Weld. J.*, 1974, **53**, 548s.
- [5] B.E. Patton: *Automat. Weld.*, 1974, **27**, 1.
- [6] C.R. Heiple and J.R. Ropper: *Weld. J.*, 1981, **60**, 143s.
- [7] C.R. Heiple and J.R. Ropper: *Weld. J.*, 1982, **61**, 97s.
- [8] Y. Takeuchi and R. Takagi and T. Shinoda: *Weld. J.*, 1992, **71**, 83s.
- [9] S.M. Gurevich and V.N. Zamkov: *Avtom. Svarka*, 1966, **12**, 13.
- [10] M. Kuo, Z. Sun and D. Pan: *Sci. Technol. Weld. Join.*, 2001, **6**, 17.
- [11] P.C.J. Anderson and R. Wiktorowica: *Weld. Met. Fabr.*, 1996, **64**, 108.
- [12] W. Lucas and D. Howse: *Weld. Met. Fabr.*, 1996, **64**, 11.
- [13] D.D. Schwemmer and D.L. Olson and D.L. Williamson: *Weld. J.*, 1979, **58**, 153s.
- [14] F. Liu, S. Lin, C. Yang and L. Wu: *Trans. Chin. Weld. Inst.*, 2002, **23**, 1.
- [15] T. Paskell, C. Lundin and H. Castner: *Weld. J.*, 1997, **76**, 57.
- [16] F. Liu, S. Lin, C. Yang and L. Wu: *Trans. Chin. Weld. Inst.*, 2002, **23**, 5.
- [17] Y. Wang and H.L. Tsai: *Metall. Mater. Trans. B*, 2001, **32**, 501.
- [18] M. Tanaka, T. Shimizu, H. Terasaki, M. Ushio, F. Koshi-ishi and C.L. Yang: *Sci. Technol. Weld. Join.*, 2000, **5**, 397.
- [19] P.J. Modenesi, E.R. Apolimario and I.M. Pereira: *J. Mater. Process. Technol.*, 2000, **99**, 260.
- [20] D. Fan, R.H. Zhang, Y.F. Gu and M. Ushio: *Trans. JWRI*, 2001, **30**, 35.
- [21] D.S. Howse and W. Lucas: *Sci. Technol. Weld. Join.*, 2000, **5**, 189.
- [22] S. Sire and S. Marya: *Proc. 7th Int. Symp., Kobe, Japan*, 2001, 113.
- [23] S. Sire and S. Marya: *Proc. 7th Int. Symp, Kobe, Japan*, 2001, 107.
- [24] S.P. Lu, H. Fujii, H. Sugiyama, M. Tanaka and K. Nogi: *Mater. Trans.*, 2002, **43**, 2926.
- [25] S.P. Lu, H. Fujii, H. Sugiyama and K. Nogi: *Metall. Mater. Trans. A*, 2003, **34**, 1901.
- [26] S. Leconte, P. Paillard and P. Chapelle: *Sci. Technol. Weld. Join.*, 2007, **12**, 120.
- [27] A. Rodrigues and A. Loureiro: *Sci. Technol. Weld. Join.*, 2005, **10**, 760.
- [28] R.H. Zhang and D. Fan: *Sci. Technol. Weld. Join.*, 2007, **12**, 15.
- [29] B.N. Bad'yanov, V.A. Davdov and V.A. Ivanov: *Avtomat. Svarka*, 1974, **6**, 1.
- [30] B.N. Bad'yanov: *Avtomat. Svarka*, 1975, **1**, 74.
- [31] C.R. Heiple and P. Burgardt: *Weld. J.*, 1985, **64**, 159s.
- [32] S.P. Lu, H. Fujii and K. Nogi: *Mater. Sci. Eng. A*, 2004, **380**, 290.
- [33] S.P. Lu, H. Fujii and K. Nogi: *Scripta Mater.*, 2004, **51**, 271.
- [34] S.P. Lu, H. Fujii and K. Nogi: *Metall. Mater. Trans.*, 2004, **35**, 2861.
- [35] S.P. Lu, H. Fujii, K. Nogi and T. Sato: *Quarterly J. Japan Welding Soc.*, 2007, **25**, 196.
- [36] M.M. Savitskii and G.I. Leskov: *Avtomat. Svarka*, 1980, **9**, 17.
- [37] H.C. Ludwig: *Weld. J.*, 1968, **47**, 234s.
- [38] T. Ohji, A. Make, M. Tamura, H. Inoue and K. Nishiguchi: *J. Jpn. Weld. Soc.*, 1990, **8**, 54.
- [39] C.R. Heiple, J.R. Roper, R.T. Stagner and R.J. Aden: *Weld. J.*, 1983, **62**, 72s.
- [40] H. Fujii, N. Sogabe, M. Kamai and K. Nogiz: *Proc. 7th Int. Symp, Kobe, Japan*, 2001, 131.
- [41] S. Leconte, P. Paillard and P. Chapelle: *Sci. Technol. Weld. Join.*, 2006, **11**, 389.
- [42] S. Leconte, P. Paillard and J. Saindrenan: *Sci. Technol. Weld. Join.*, 2006, **11**, 43.
- [43] J.J. Lowke, M. Tanaka and M. Ushio: *57th Annual Assembly of International Institute of Welding, Osaka, Japan*, 2004, IIW Doc.212-1053-04.
- [44] S.P. Lu, H. Fujii, K. Nogi and T. Sato: *Sci. Technol. Weld. Join.*, 2007, **12**, 689.
- [45] S.P. Lu, H. Fujii and K. Nogi: *J. Mater. Sci.*, 2008, **43**, 4583.
- [46] C. Limmaneevichitr and S. Kou: *Weld. J.*, 2000, **79**, 231s.
- [47] S. Kou and D.K. Sun: *Metall. Trans. A*, 1985, **16**, 203.
- [48] S. Kou and Y.H. Wang: *Weld. J.*, 1986, **65**, 63s.
- [49] P. Sahoo, T. Debroy and M.J. Mcnallan: *Metall. Trans. B*, 1988, **19**, 483.
- [50] H. Taimatsu, K. Nogi and K. Ogino: *J. High Temp. Soc.*, 1992, **18**, 14.